

An Integrated Nonlinear Placement Framework with Congestion and Porosity Aware Buffer Planning

Tung-Chieh Chen*
Graduate Institute of
Electronics Engineering
National Taiwan University
Taipei 106, Taiwan

Ashutosh Chakraborty
Department of Electrical &
Computer Engineering
University of Texas at Austin,
TX 78712

David Z. Pan
Department of Electrical &
Computer Engineering
University of Texas at Austin,
TX 78712

donnie@eda.ee.ntu.edu.tw ashutosh@cerc.utexas.edu dpan@ece.utexas.edu

ABSTRACT

Due to skewed scaling of interconnect versus cell delay in deep submicron CMOS, modern VLSI timing closure requires extensive buffer insertion. Inserting a large number of buffers may cause not only dramatic cell migration but also routing hotspots. If buffering is not controlled well, it may fail to close a design. Placement with buffer porosity (i.e., cell density) awareness can allocate space for inserting these buffers, and buffering with congestion awareness can improve the routability. Therefore, there is essential need for a placement framework with explicit porosity and congestion control. In this paper, we propose the first integrated nonlinear placement framework with porosity and congestion aware buffer planning. We demonstrate the integration of increasingly refined cell porosity and routing congestion aware buffer planning and insertion methodology in a high quality nonlinear placer. Our experiments show the improvement of average routing overflow by 69%, average wirelength by 28% and average buffer count by 40%, compared with the traditional placement framework without buffer planning.

Categories and Subject Descriptors: B.7.2 [Integrated Circuits]: Design Aids

General Terms: Algorithms, Design, Performance

Keywords: VLSI, Physical Design, Placement, Buffer

1. INTRODUCTION

Interconnect optimization is critical in the modern physical design closure flow since interconnect delay now dominates gate delay, and its importance will keep increasing as we further reduce feature sizes. Buffers insertion is a widely used technique to tackle this increasing interconnect delay. Optimal insertion of buffers in an interconnect reduces its delay dependence on length from a quadratic function to a

*The work of T.-C. Chen was carried out while he was a visiting Ph.D. student at Univ. of Texas at Austin in 2007.

Permission to make digital or hard copies of all or part of this work for personal or classroom use is granted without fee provided that copies are not made or distributed for profit or commercial advantage and that copies bear this notice and the full citation on the first page. To copy otherwise, or republish, to post on servers or to redistribute to lists, requires prior specific permission and/or a fee.

DAC 2008, June 8–13, 2008, Anaheim, California, USA
Copyright 2008 ACM 978-1-60558-115-6/08/0006...5.00

linear function. For each technology node and a given routing layer, there exists some optimal distance, called buffer insertion length (BIL), such that placing buffers separated by BIL along an interconnect minimizes the delay through it. It is known that with each technology node global interconnects do not scale (actually may even become longer), intermediate interconnects can scale by 0.7X, but the buffer insertion length (BIL) scales by 0.58X [15]. Therefore, the number of buffers required on an (scaled) intermediate interconnect increases by 1.2X whereas for global interconnects, it increases by nearly 1.8X for each technology node.

It is predicted that the number of buffers may approach 70% at the 32nm technology node [17]. Without controlling the cell *porosity*, there may be not enough space for inserting buffers. Therefore, the placement by the traditional placement algorithm may cause buffer number explosion [16]. The number of buffers can explode as follows: Insertion of a large number of buffers creates a lot of overlaps with existing cells. Removing these overlaps during legalization causes the placement to change drastically, introducing new critical paths. To satisfy timing requirements on these new critical paths, buffer insertion can be applied to them, but the legalization of these new buffers may require many existing cells or buffers be moved from their original positions, invalidating the timing achieved by earlier buffer insertion leading to even more additional buffers.

Another critical impact of buffer insertion of long interconnects is the loss of flexibility available to a router which can increase the routing *congestion*. Modern routers are overwhelmed by requirements to satisfy electrical connectivity, timing, wire density, crosstalk, and other objectives. As a long net has much more flexibility to be routed as compared to a sequence of short nets, buffer insertion, which breaks an interconnect into several shorter interconnects, reduces the flexibility available to the router. Also, since typical interconnect structures are trees (with only one path from source to each sink), the connectivity constraint for a router is a hard requirement without which the chip will not function.

To overcome the possible buffer number explosion and routing bottlenecks, there is critical need for a framework for integration of buffer insertion considering routing congestion *during* placement. Such a framework should start planning the buffers at early stage and follow through its planning until the final stage of placement. This work presents the first framework of this kind — we integrate increasingly refined routing congestion aware buffer estimation and

planning technique in a high quality nonlinear placer. Our framework shows promising results, and is able to reduce the average buffer numbers by 40%, average routing overflows by 69% and average wirelength by 28% compared with the traditional placement without buffer planning.

The rest of this paper is organized as follows: Section 2 discusses the previous work and our main technical contributions. We present a brief background on placement, routing congestion and buffer insertion in Section 3. Section 4 presents our problem formulation and the proposed framework. We demonstrate the efficacy of our approach with results in Section 5. Section 6 concludes our paper.

2. PREVIOUS WORKS AND OUR CONTRIBUTIONS

There are some previous works handling buffer insertion during the placement. However, none of them consider the routing congestion. As will be shown shortly, this is a major drawback because the impact of buffer insertion on routability can be huge, especially at lower technology nodes where the buffer number is predicted to be very high.

Saxena and Halpin proposed an integrated buffer insertion and placement flow by modeling buffers explicitly based on a Kraftwerk-like quadratic placement flow [16]. Goplen et al. further extended their flow using net weighting to reduce the buffer counts [9]. Luo et al. proposed an integrated buffer insertion and placement flow by modeling buffers as dummy blocks that does not involve in quadratic placement and re-inserting buffers into new positions for each placement iteration [13]. Jahanian and Zamani proposed a buffer planning algorithm for the floor-placement design flow by creating a buffer requirement map and moving the whitespace by the detailed placement based on the map [10].

Unlike those previous works, we present a new integrated nonlinear placement framework with porosity and congestion aware buffer planning. Given a circuit, our placer finds the desired positions for all cells and reserves whitespace for buffers in their most probable insertion location during the placement process. In addition, our framework analyzes the buffer count and their locations at various levels of granularity and minimizes the wirelength and the routing congestion at the same time. Our main technical contributions are:

- We propose the first simultaneous buffer planning and placement framework which is aware of routing congestion, integrated in a nonlinear placement framework.
- We propose and apply several increasingly finer granularity buffer density estimation techniques to guide the global placement to intelligently reserve whitespace for buffer insertion. This approach smoothly spreads the cells and buffers and converges to a desired placement.
- The Steiner tree topology is considered during the placement and the buffer insertion algorithm. Use of Steiner tree gives us a quick peek at the possible routing scenario and adjust the placement accordingly, leading to better routability.

3. PRELIMINARIES

In this section, we review the nonlinear analytical placement method, buffer insertion, and routing congestion.

3.1 Nonlinear Placement

We use a hypergraph $H = (V, E)$ to model a circuit. Let vertices $V = \{v_1, v_2, \dots, v_n\}$ represent cells, and hyperedges $E = \{e_1, e_2, \dots, e_m\}$ represent nets. Let x_i and y_i be the x and y coordinates of the center of cell v_i , respectively.

The analytical placement approach optimizes wirelength under the density constraint. The uniform non-overlapping bin grid model for the placement region is used to model the density constraint. Therefore, the global placement problem can be formulated as a constrained minimization problem as follows:

$$\begin{aligned} \min \quad & W(V, E) \\ \text{s.t.} \quad & D_{cell}(V) \leq D_{grid}, \quad \text{for each bin grid,} \end{aligned} \quad (1)$$

where $W(V, E)$ is the wirelength function, $D_{cell}(V)$ is the cell area function in bins, and D_{grid} is the total area allowed in a bin. The wirelength $W(V, E)$ is defined as the total half-perimeter wirelength (HPWL). Since $W(V, E)$ is not smooth, it is hard to minimize it directly. We apply the log-sum-exp function [11, 14], which is one of the most effective and efficient function for HPWL approximation. The cell area in a bin can be computed by the horizontal overlap multiplies the vertical overlap. We use the bell-shaped function [11, 14] to smooth the overlap function.

To solve Eqn. (1), we use the quadratic penalty method, implying that we solve a sequence of unconstrained minimization problems of the form

$$\min \quad W(V, E) + \lambda \sum_{\forall bin} (D_{grid} - D_{cell})^2 \quad (2)$$

with increasing λ 's. The solution of the previous problem is used as the initial solution for the next one.

3.2 Buffer Insertion

Buffer insertion is usually applied in an iterative fashion. Given a placement, we compute the failing paths in a design, insert buffers to desired positions to fix timing, and remove overlaps caused by buffers. The resulting placement is then analyzed again for timing, and additional buffers may need to be inserted. The insertion step iteratively continues until the timing is satisfied. However, as the buffer count increases rapidly with process scaling, this approach does not work since the newly introduced buffers create too many placement overlaps and the placement cannot be legalized without significant placement perturbation. Such a large placement perturbation generates new timing critical paths which need to be buffered again, leading to a possibly never ending loop.

On a hypernet, buffer insertion can be done for different objectives such as maximizing the worst (among all sinks of the hypernet) negative slack, minimizing the delay of the most critical sink, minimizing the delay of all the sinks, or bounding the maximum slew rate of the signal. Since the primary focus of this work is not the comparative study of pros/cons of different buffering objectives, in this work we applied buffer insertion for minimizing the delay of all the sinks of a failing hypernet as well as for hypernets for which slew is more degraded than allowed by the library.

3.3 Routing Congestion and Buffers

With a large number of buffers on a chip, placement of these buffers may determine the ease of routing of each net.

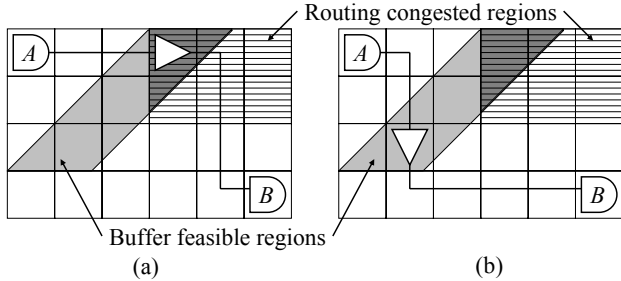


Figure 1: (a) The buffer position causes higher routing congestion. (b) Another buffer position does not increase routing congestion.

Buffer insertion restricts the flexibility of different routes for a net. Buffer insertion divides the net into several smaller net segments, and router usually route them independently. Therefore, a bad buffer insertion position may cause routing go through high routing congestion areas. We give an example in Figure 1. The regions with horizontal lines have higher routing congestion. The gray parallelogram is the region in which a placement of buffer satisfies the delay constraint between cells A and B . If the buffer is placed inside the routing congested region, Figure 1(a), the router cannot avoid going through this region since the net terminal is located in it. In contrast, if we place the buffer outside the congested region, Figure 1(b), we can avoid the net from going through the congested region thus relieving the routing congestion.

4. PROPOSED FRAMEWORK

4.1 Formulation

To deal with increasing buffer count, the placement formulation needs to consider the cell/buffer porosity and routing congestion during the placement. We have the new formulation for the placement with buffer density as follows,

$$\begin{aligned} \min \quad & W(V, E) \\ \text{s.t.} \quad & D_{cell}(V) + D_{buf}(V, E) \leq D_{grid}, \end{aligned} \quad (3)$$

where $W(V, E)$ is total half-perimeter wirelength of all nets, D_{cell} is the area of cells, D_{buf} is the area of buffers, and D_{grid} is the area of the bin grids.

The buffer density D_{buf} is computed based on the current placement. All timing failing nets that are longer than the buffer insertion length (BIL) need to be buffered. A static timing and slew analyzer can be used to find the nets that need to be buffered, and the BIL is computed according to the given technology parameters. The buffer density map provides the possible buffer insertion positions and guides global placement to reserve enough whitespace for buffer insertion. Considering a source-sink net in Figure 2(a), we can compute optimal buffer insertion positions using the BIL. We can apply the two-dimensional *Feasible Region* from [8]. The feasible region is defined as the region where the buffer may be located such the delay constraint can be satisfied by inserting the buffer into any location in that region. It is shown that even under very tight timing constraint, say, 10% more delay from the optimal delay, the feasible region can be as much as 50% of the wire length. An example of the two-dimensional feasible region is shown in Figure 2(a),

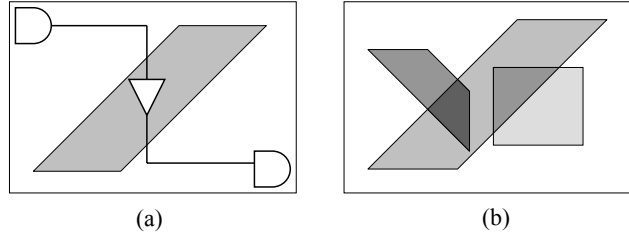


Figure 2: (a) Using the feasible region to the compute the buffer density. (b) The buffer density map is derived from the summation of all predicted buffer density regions.

which provides a lot of flexibility to plan buffer locations while minimizing routing congestion. The buffer density map is obtained by summing up all possible buffer regions, as shown in Figure 2(b).

We resort to the quadratic penalty method to solve Eqn. (3):

$$\min \quad W + \lambda \sum_{\forall bin} (D_{grid} - D_{cell} - D_{buf})^2. \quad (4)$$

To efficiently solve the unconstrained problem in Eqn. (2), we apply the conjugate gradient (CG) method with controlling the step size dynamically [6]. During each iteration, we update the buffer density D_{buf} based on current placement and the given buffering model. Inserting buffers does not effect HPWL because we always allocate buffers inside the bounding box of the net. With gradually increasing λ and the cells are spread with necessary buffer space allocated. As a result, we can find a desired placement with the optimal wirelength that does not violate density constraints. Further, since the buffer density is constructed using a congestion-aware method, the resulting routing overflows can be reduced effectively.

4.2 Buffering Model

To pro-actively estimate buffer insertion positions, the ideal way is to call the router and get the net topology and the routing congestion. However, such a flow would be exceedingly slow. The buffering step is performed many times during the placement, and thus only faster models can be applied. We introduce the following four buffering models. See Figure 3(b), (c), (d), and (e) for the illustrations of the corresponding models.

- **HPWL.** The half-perimeter wirelength (HPWL) divided by the buffer insertion length (BIL) is used to obtain the required buffer number. The buffer density inside the wire bounding box in this stage is

$$\frac{(w_{bb,i} + h_{bb,i})/l_{crit} - t_i}{w_{bb,i}h_{bb,i}}, \quad (5)$$

where $w_{bb,i}$ ($h_{bb,i}$) is the width (height) of the bounding box of net i , l_{crit} is the BIL, and t_i is the number of the terminals for net i .

- **StWL.** Steiner wirelength is used to computed the buffer number. The buffer density inside the wire bounding box is

$$\frac{s_i/l_{crit} - t_i}{w_{bb,i}h_{bb,i}}, \quad (6)$$

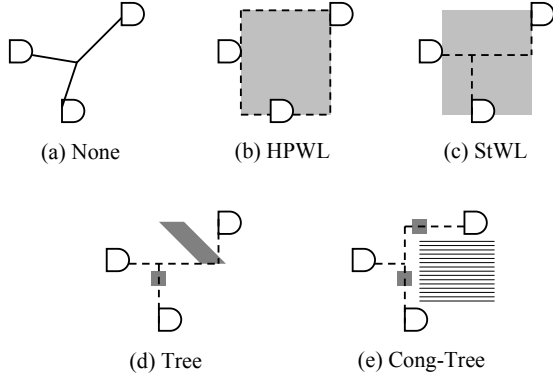


Figure 3: Five different levels of buffer density computation. The shading regions are buffer density region. (a) Pure wirelength-driven placement without buffering. (b) Using HPWL. (c) Using Steiner wirelength. (d) Using Steiner tree. (e) Using Steiner tree with congestion consideration.

where s_i is the Steiner wirelength of net i . The migration from HPWL to Steiner wirelength improves the accuracy of the number of buffers. Since buffer prediction is performed during placement many times, we need a fast yet accurate Steiner wirelength calculation method, such as FLUTE [7]. Note that our implementation is not limited any particular Steiner tree generation tool because at this stage we only use the Steiner wirelength.

- **Tree.** Based on the Steiner tree topology, the buffering map is computed using the feasible regions of buffers while traversing the Steiner tree based on the buffer insertion length. This gives the most accurate estimate of number of buffers and their possible positions.
- **Cong-Tree.** Based on the Steiner tree topology, we use the probabilistic routing model [12, 18] to estimate the routing congestion. Then, we consider the possible routing paths through the feasible regions and pick a path which contribute the least congestion.

Although the tree models are more accurate than wire length models, the placement process may become very slow because of Steiner tree construction. Therefore, instead of directly using the Steiner tree for buffering and congestion consideration, we propose to use the MIX model, a sequence of five stages with increasingly accurate estimation and smoothly spreading the cell during the placement.

At first stage, a pure wirelength-driven placer without buffer planning is used to obtain a rough placement. Since cell positions changes very fast during this stage, the buffer requirements and congestion are hard to estimate accurately. As the placement iteration increases, we gradually change to more accurate models, HPWL, StWL, Tree, and Cong-Tree, for each stage to compute buffer density, see Figure 4. Between each stage, we analyze the timing according to latest cell coordinates. During the final stage of our placement flow we *actively* place the buffer in low congested region.

4.3 Our Flow

Figure 5 gives our placement flow. First, we find a rough placement by solving the wirelength-driven placement prob-

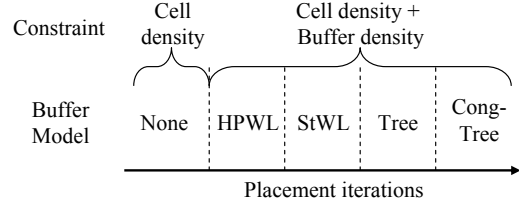


Figure 4: The MIX model. Buffering model changes as the placement iteration increases. This approach can smooth the buffer density function and spend much shorter runtime compared with using Cong-Tree alone.

```

01. // Obtain a rough placement.
02. Cluster cells to obtain the clustered netlist;
03. Minimize  $W + \lambda \sum (D_{grid} - D_{cell})^2$ ;
04. Decluster cells to get a rough placement;
05.  $ite = 0$ ;
06. // Continue placement with buffer planning.
07. do
08.      $ite = ite + 1$ ;
09.     Select a model according to  $ite$ ;
10.     Analyze the current timing;
11.     //Minimize  $W + \lambda \sum (D_{grid} - D_{cell} - D_{buf})^2$ .
12.     do
13.         if( buffering model == CongTree )
14.             Update the congestion map;
15.             Update cell density and buffer density;
16.             Compute the conjugate gradient direction;
17.             Update current cell positions;
18.         until (the minimal value is found);
19.         Increase  $\lambda$  by 2;
20.     until (there is no area overflow in bins or
21.           the placement is converged);
22.     Insert buffers into desired positions;
23.     Legalize the placement;
24. return netlist and cell/buffer positions;

```

Figure 5: Our placement flow.

lem in the clustered level. We cluster cells using the best-choice clustering algorithm [5]. Then, all cluster positions are obtained by minimizing the function $W + \lambda \sum (D_{grid} - D_{cell})^2$. After declustering, we obtain a rough placement.

Then, we enter the loop to further optimize wirelength with buffer planning. In each iteration, we select a buffering model and analyze timing to get the latest timing information to determine which nets to be buffered. Then, we find the desired placement by minimizing the objective function $W + \lambda \sum (D_{grid} - D_{cell} - D_{buf})^2$. The conjugate gradient method with dynamic step size method is applied, and the buffer density map D_{buf} is updated inside the conjugate gradient loop. If the buffering model Cong-Tree is used, we also need to update the routing congestion map during the placement. The placement iteration continues until all required buffer space are allocated, and there is no or little density overflows in each bin. Then, we insert buffers into the pre-allocated buffer space, and the placement is legalized and all overlaps are removed. Finally, we return the modified netlist and all cell/buffer positions.

5. EXPERIMENTAL RESULTS

We implemented the proposed nonlinear placement framework in C++, and all the experiments were conducted on a 3.40GHz Intel Pentium 4 machine. OpenAccess [2] and

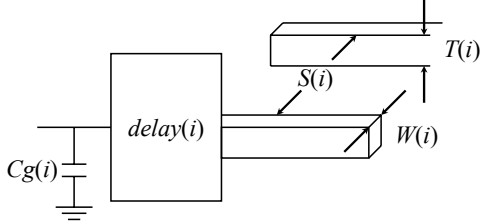


Figure 6: Parameters of the cell library. $X(i)$ is the value of parameter X for technology node i . Cg , S , T and W represents gate input capacitance, interwire spacing, interconnect height and interconnect width. $Delay$ represents the delay through a cell.

OAGear timer [3] are used for our experiments. By default the OAGear timer uses a linear delay model (i.e., it assumes optimal buffer insertion has been done on each net), but since our aim is to quantify the impact of buffer planning/insertion, we modified the OAGear timer to compute the Elmore delay.

We tested our proposed placement framework on five OpenCores circuits¹ [1,4]. The benchmark statistics are shown in Table 1. We set the chip utilization rate to 60%. By doing so, we can focus on the effects of different buffer planning methods and minimize the possibility of failing to remove overlaps by the legalizer. Because our nonlinear placement framework does not evenly distribute cells to the whole chip, using low utilization rate does not harm the resulting wirelength at all.

In order to model wiring and placement complexity at 32nm process technology nodes, we used unshrunk cells along with shrunk inter-repeater distances. The work in [16] experimentally observed that this method of analysis successfully lower-bounds future technology node’s buffer insertion problem. Figure 6 represents the state of a library gate and interconnect parameter at a particular technology node i . We used the following equations to advance the technology node from Cadence CRETE 180nm library down to 130nm, 90nm, 65nm, 45nm, and 32nm.

$$\begin{aligned}
 delay(i+1) &= delay(i) * 0.8; \\
 Cg(i+1) &= Cg(i) * 0.5; \\
 T(i+1) &= T(i) * 0.8; \\
 W(i+1) &= W(i) * 0.8; \\
 S(i+1) &= S(i) * 0.8.
 \end{aligned}
 \tag{7}$$

Using these geometrical parameters, we calculated the scaling factor for other parameters such as sheet resistance, sheet capacitance, edge capacitance and via resistances and re-built the Liberty format which was read in by the placer and the OAGear timer.

Two experiments were conducted. First, we compared different buffering models. Second, three different placement approaches were evaluated. The same iterative buffer insertion method was applied to all placement results: we computed the failing paths in a design, inserted buffers to desired positions to fix timing, and removed overlaps caused by buffers. These three step were iteratively performed until

¹Since the OAGear timer could not handle tri-state nets and it crashed in some OpenCores circuits, we selected five larger circuits from OpenCores that OAGear timer can work correctly.

Table 1: Benchmark statistics.

Circuit	Cell #	Net #	Pin #
des_area	4881	5122	304
tv80	7161	7179	46
systemcaes	7959	8220	389
aes_core	20795	21055	388
des_perf	98341	98576	298

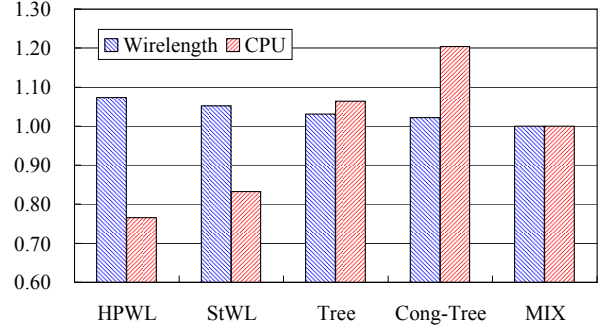


Figure 7: The normalized wirelengths and CPUs for different buffering models.

the timing was met or the iteration had been executed for 10 times, and the final results are reported.

5.1 Buffering Model Comparison

In the first experiment, we compare the four buffering models, HPWL, StWL, Tree, and Cong-Tree, with our progressive mixed model (MIX), which was introduced in Section 4.2. We use our placement framework integrated with these five different models individually to obtain the placement CPU times and the final wirelengths after buffer insertion. The average wirelength and the CPU time are plotted in Figure 7. All results are normalized to those using our MIX model. It is clear that a more accurate model can lead to shorter resulting wirelength but with longer placement CPU time. Our MIX model results in the shortest average wirelength, which is 8%, 5%, 3%, and 2% lesser than those by HPWL, StWL, Tree, and Cong-Tree models, respectively. This reveals the importance of smoothing the buffer density function gradually instead of using the most accurate model (Cong-Tree) in the nonlinear placement framework. The average CPU time of the MIX model is right at the middle. These results show that our MIX model can effectively reduce the wirelength while spending moderate CPU time.

5.2 Results of Different Placement Approaches

In the second experiment, we compare three different placement approaches: (1) placement without buffer planning, (2) integrated placement with porosity aware buffer planning, and (3) integrated placement with porosity and congestion aware buffer planning. Table 2 gives the resulting buffer counts, wirelengths, routing overflows, and CPU times. The buffer count is the total number of buffers after iterative buffer insertion; the wirelength is the final HPWL of the modified netlist; the overflow value is reported using the probabilistic routing model [12,18], which has high correlation with various routers and is also used in many routers; the CPU time is only for the placement part, excluding the time for iterative buffer insertion. The last row

Table 2: The results of different approaches.

Circuit	Without Buffer Planning				Integrated Flow (Poro.)				Integrated Flow (Poro. + Cong.)			
	Buf #	Wire-length	Over-flow	CPU (sec)	Buf #	Wire-length	Over-flow	CPU (sec)	Buf #	Wire-length	Over-flow	CPU (sec)
des_area	1755	9.00 e8	8265	5	771	5.47 e8	347	16	741	5.41 e8	368	18
tv80	926	8.22 e8	407	12	889	8.17 e8	368	18	884	8.12 e8	216	34
systemcaes	785	1.13 e9	1524	10	703	1.11 e9	1430	29	703	1.11 e9	1389	37
aes_core	12437	5.09 e9	70626	43	13894	5.77 e9	97033	103	4510	2.86 e9	3790	117
des_perf	67115	2.71 e10	390117	514	26261	1.24 e10	23385	1007	25813	1.24 e10	12880	1497
Comp.	1.00	1.00	1.00	1.00	0.76	0.83	0.66	2.39	0.60	0.72	0.31	3.15

in Table 2 reports the average values that are normalized to those without buffer planning.

Compared with the placement without buffer planning, the integrated flow with porosity aware buffer planning reduces the average buffer count by 24%, the average wirelength by 17%, the average routing overflow by 34%. The CPU time is around 2.39X. Compared with the integrated flow with only porosity awareness, the integrated flow with porosity and congestion awareness can further reduce the average buffer count by 16%, the average wirelength by 11%, the average routing overflow by 35%. The CPU time penalty is due to the routing congestion analysis and the congestion aware buffering model during the placement. Although the placement CPU time itself is 3.15X, the resulting placement has much less routing overflows that may significantly reduce the routing time. The results show that our proposed integrated framework with porosity and congestion aware buffer planning can effectively obtain high quality placement results.

6. CONCLUSIONS

In this work, we presented the first integrated nonlinear placement framework with porosity and congestion aware buffer planning. Our framework performs buffer planning starting from very early global placement stages, followed by increasingly accurate buffering models and congestion estimation. We validated our framework for several OpenCores benchmarks at the projected 32nm technology node and demonstrated significant improvement in design closure process using metric such as number of buffers, wirelength, and routing overflows.

Our future work will be targeted in two directions. We would like to explore buffer insertion for other objectives (rather than for minimizing the delay to each sink of a hypernet). We would also like to exploit the methodology of using the sequence of increasingly accurate whitespace requirement for other related issues such as simultaneous gate sizing and placement.

7. ACKNOWLEDGMENTS

We would like to thank Prof. Yao-Wen Chang from National Taiwan University for helpful discussions. This research is supported in part by SpringSoft, Inc., National Science Council of Taiwan under Grant No's NSC 96-2221-E-002-245, NSC 96-2628-E-002-248-MY3, NSC 96-2628-E-002-249-MY3, NSC 96-2752-E-002-008-PAE, NSC 96-2917-I-002-031, NSF Career Award CCF-0644316, SRC under contract TJ-1321, IBM Faculty Award, and Intel equipment donations.

8. REFERENCES

- [1] *IWLS 2005 Benchmarks*. <http://iwls.org/iwls2005/benchmarks.html>.
- [2] *OpenAccess*. <http://www.si2.org/>.
- [3] *OpenAccess Gear*. <http://opendatools.si2.org/oagear/>.
- [4] *OpenCores*. <http://www.opencores.org/>.
- [5] C. Alpert, A. Kahng, G.-J. Nam, S. Reda, and P. Villarrubia. A semi-persistent clustering technique for VLSI circuit placement. In *Proc. ACM Int. Symp. on Phys. Des.*, pages 200–207, San Francisco, CA, Apr. 2005.
- [6] T.-C. Chen, Z.-W. Jiang, T.-C. Hsu, and Y.-W. Chang. A high-quality mixed-size analytical placer considering preplaced blocks and density constraints. In *Proc. IEEE/ACM Int. Conf. on Comput.-Aided Des.*, San Jose, CA, Nov. 2006.
- [7] C. Chu and Y.-C. Wong. Fast and accurate rectilinear steiner minimal tree algorithm for vlsi design. In *Proc. ACM Int. Symp. on Phys. Des.*, pages 28–35, 2005.
- [8] J. Cong, T. Kong, and Z. D. Pan. Buffer block planning for interconnect planning and prediction. *IEEE Trans. VLSI Syst.*, 9(6):929–937, 2001.
- [9] B. Goplen, P. Saxena, and S. Sapatnekar. Net weighting to reduce repeater counts during placement. In *Proc. ACM/IEEE Des. Autom. Conf.*, pages 503–508, Anaheim, CA, June 2005.
- [10] A. Jahanian and M. S. Zamani. Improved timing closure by early buffer planning in floor-placement design flow. In *Proc. ACM Great Lakes Symp. on VLSI*, pages 558–563, Stresa-Lago Maggiore, Italy, Mar. 2007.
- [11] A. B. Kahng and Q. Wang. Implementation and extensibility of an analytic placer. *IEEE Trans. Computer-Aided Design*, 24(5), May 2005.
- [12] J. Lou, S. Thakur, S. Krishnamoorthy, and H. S. Sheng. Estimating routing congestion using probabilistic analysis. *IEEE Trans. Computer-Aided Design*, 21(1):32–41, Jan. 2002.
- [13] L. Luo, Q. Zhou, Y. Cai, X. Hong, and Y. Wang. A novel technique integrating buffer insertion into timing driven placement. In *Proc. IEEE Int. Symp. on Circuits and Systems*, Island of Kos, Greece, May 2006.
- [14] W. C. Naylor, R. Donnelly, and L. Sha. US patent 6,301,693: Non-linear optimization system and method for wire length and dealy optimization for an automatic electric circuit placer. 2001.
- [15] J. M. Rabaey, A. Chandrakasan, and B. Nikolic. *Digital Integrated Circuits*. Prentice Hall, 2 edition, 2002.
- [16] P. Saxena and B. Halpin. Modeling repeaters explicitly within analytical placement. In *Proc. ACM/IEEE Des. Autom. Conf.*, pages 699–704, San Diego, CA, June 2004.
- [17] P. Saxena, N. Menezes, P. Cocchini, and D. Kirkpatrick. Repeater scaling and its impact on cad. *IEEE Trans. Computer-Aided Design*, 23(4):451–463, 2004.
- [18] J. Westra, C. Bartels, and P. Groeneveld. Probabilistic congestion prediction. In *Proc. ACM Int. Symp. on Phys. Des.*, pages 204–209, Phoenix, AZ, 2004.